Appl. Magn. Reson. 3, 1–18 (1992)

Applied Magnetic Resonance

ENDOR Studies of Alkyl Substituted p-Benzosemiquinones in Reversed Micelles and in 2-Propanol

B.Kirste, D.Niethammer, P.Tian and H.Kurreck

Institut für Organische Chemie der Freien Universität Berlin, Berlin, Germany

Received September 12, 1991

Abstract. Various substituted p-benzosemiquinone radical anions, inter alia ubisemiquinone and derivatives, have been investigated in 2-propanol and in reversed micelles by EPR and ENDOR spectroscopy. Unsymmetrical semiquinones, with respect to the oxygen atoms, experience remarkable hyperfine shifts depending on the medium. This effect even allows differentiation between stereoisomers. Immobilization of the semiquinone molecules at the water-surfactant interface in reversed micelles gives rise to pronounced asymmetric linewidth effects. In the case of 2-cyclohexyl-3-methyl-1,4-benzosemiquinones, mixtures of two species (conformers) have been observed.

1. Introduction

Quinones are known to fulfil unique functions in electron transfer and natural energy conserving systems. Particularly, all green plants have ubiquinones in their mitochondria. Quinones play the role of electron acceptors during the light-induced charge separation in the primary process of photosynthesis in green plants as well as in photosynthetic bacteria [1]. Hence they are also of utmost interest as constituents of biomimetic model compounds for photosynthetic reaction centers, which are made up of quinones covalently linked to porphyrins [2]. A detailed knowledge of the geometric and electronic structure of naturally occurring semiquinone anion radicals as well as their synthetic analogs is a necessary prerequisite for a better understanding of the photoinduced electron transfer process.

Since the quinones are embedded in the thylakoid membrane of the natural photosynthetic reaction center, it would be highly desirable to study these compounds in a membrane-like environment. Actually it has turned out that reversed micelles are well suited for that purpose [3]. In contrast to normal micelles ("oil-in-water"), reversed micelles (also called inverse micelles) are

"water-in-oil" microemulsions consisting of an internal aqueous microphase (water pool) surrounded by a surfactant layer and the external organic phase [4]. These media offer the additional advantage that the solutions of the semiquinone anion radicals are more stable than those in alcoholic solvents.

In the present paper we report on a detailed EPR and ENDOR study of ubisemiquinone and a series of related synthetic semiquinones in reversed micelles and in ordinary (isotropic) solutions. Particular emphasis is given to any differences observed in these solvent systems, regarding the geometry of the radicals, their mobility, and the distribution of the unpaired electron spin.

2. Experimental

2.1. Preparation of Quinones

Some of the quinones investigated in this study are commercially available; ubiquinone-0 (**13**) was obtained from Lancaster Synthesis, ubiquinone-10 (**14**) from Serva. The other quinones were prepared by alkylation according to the method of Jacobsen and Torssell [5] via oxidative decarboxylation of carboxylic acids [3]. Isomers were separated by HPLC, structures were determined by NMR, allowing unequivocal assignments even of diastereomers (*cis*/*trans* isomers of 1,4-disubstituted cyclohexanes).

2.1.1. (4-Methoxycarbonylcyclohexyl)-methyl-1,4-benzoquinones **10c, 10t, 11c, 12t**

2-Methyl-1,4-benzoquinone (50 mmol) and cyclohexane-1,4-dicarboxylic acid monomethyl ester (70 mmol) were dissolved in a mixture of CH_2Cl_2 and water at 45°C. The oxidants $AgNO_3$ (8 mmol) and $(NH_4)_2S_2O_8$ (75 mmol) were added with stirring. After gas evolution had stopped, the organic phase was separated, dried over Na_2SO_4, and the solvent was removed. The crude product was extracted with n-pentane, yield 48 % of a mixture of several isomers. Four of these isomers were separated by HPLC (silica gel 60, column 32 × 250 mm, 100 % CH_2Cl_2). **12t**: m.p. 90–91°C; $m/z = 262$ (M^+); ^{1}H-NMR ($CDCl_3$) $\delta = 1.50$ ppm (2H, m, ax), $\delta = 1.64$ ppm (2H, m, eq), $\delta = 1.97$ ppm (2H, m, ax), $\delta = 2.07$ ppm (3H, s), $\delta = 2.09$ ppm (2H, m, eq), $\delta = 2.42$ ppm (1H, m, ax), $\delta = 2.72$ ppm (1H, m, ax), $\delta = 3.70$ ppm (3H, s), $\delta = 6.64$ ppm (2H, AB). **10t**: m.p. 96°C; $m/z = 262$ (M^+); ^{1}H-NMR ($CDCl_3$) $\delta = 1.32$ ppm (2H, m, ax), $\delta = 1.66$ ppm (2H, m, eq), $\delta = 1.93$ ppm (2H, m, ax), $\delta = 2.05$ ppm (3H, d), $\delta = 2.13$ ppm (2H, m, eq), $\delta = 2.38$ ppm (1H, m, ax), $\delta = 2.77$ ppm (1H, m, ax),

$\delta = 3.75$ ppm (3H, s), $\delta = 6.56$ ppm (1H, d), $\delta = 6.65$ ppm (1H, q). **10c**: m.p. 117°C; $m/z = 262$ (M^+); ^{1}H-NMR ($CDCl_3$) $\delta = 1.38$ ppm (2H, m, ax), $\delta = 1.66$ ppm (4H, m, ax/eq), $\delta = 2.06$ ppm (3H, d), $\delta = 2.23$ ppm (2H, m, eq), $\delta = 2.73$ ppm (2H, m, ax/eq), $\delta = 3.72$ ppm (3H, s), $\delta = 6.52$ ppm (1H, d), $\delta = 6.60$ ppm (1H, q). **11c**: m.p. 92°C; $m/z = 262$ (M^+); ^{1}H-NMR ($CDCl_3$) $\delta = 1.42$ ppm (2H, m, ax), $\delta = 1.65$ ppm (4H, m, ax/eq), $\delta = 2.06$ ppm (3H, d), $\delta = 2.24$ ppm (2H, m, eq), $\delta = 2.76$ ppm (2H, m, ax/eq), $\delta = 3.70$ ppm (3H, s), $\delta = 6.46$ ppm (1H, d), $\delta = 6.56$ ppm (1H, q).

15, **16c** and **16t** were prepared analogously from 2,3-dimethoxy-5-methyl-benzoquinone; details will be reported elsewhere [6].

2.1.2. 2-Methyl- and 2,3-dimethyl-5-phenyl-1,4-benzoquinone **6**, **7**

Diphenylcadmium was prepared by adding a suspension of $CdCl_2$ or CdI_2 (10 mmol) in diethyl ether to phenylmagnesium bromide, obtained from bromobenzene (20 mmol) and Mg (25 mmol) in diethyl ether under inert gas [7]. This solution was added dropwise to a solution of the respective quinone (10 mmol of 2-methyl-1,4-benzoquinone or 2,3-dimethyl-1,4-benzoquinone) in diethyl ether. The mixture was refluxed until the color changed from blue to green or yellow. Work-up by cooling with ice, acidification with dilute HCl or a saturated solution of NH_4Cl, separation of the organic phase, drying over Na_2SO_4, removal of the ether and extraction of the residue with n-pentane. The yellow crude product was recrystallized from ethanol. **6**: 45 % yield; m.p. 110°C; $m/z = 198$ (M^+); ^{1}H-NMR ($CDCl_3$) $\delta = 2.12$ ppm (3H, d), $\delta = 6.72$ ppm (1H, q), $\delta = 6.88$ ppm (1H, s), $\delta = 7.48$ ppm (5H, m). **7**: 40 % yield; m.p. 98°C; $m/z = 212$ (M^+); ^{1}H-NMR ($CDCl_3$) $\delta = 2.08$ ppm (3H, s), $\delta = 2.12$ ppm (3H, s), $\delta = 6.82$ ppm (1H, s), $\delta = 7.44$ ppm (5H, m).

2.2. Sample Preparation

Reversed micelles were prepared with cyclohexane/2-methyl-2-hexanol (5:1) as organic solvent. Cetyltrimethylammonium bromide (CTAB) was used as cationic surfactant in concentrations of 0.2 to 0.3 mol/l. Stock solutions were stored under argon. Aqueous solution (usually 1 M KOH, 1 M KBr) was added in the proper amount to give the desired W_0-value of 10 to 15; W_0 is defined as the ratio of molar concentrations [water]/[surfactant]. The formation of reversed micelles was accelerated by ultrasonification. The respective quinone was added as solid, and the remaining oxygen was removed by shortly flushing the solution with argon. A trace of benzoin was added as reductant in the case of ubiquinone and derivatives, otherwise

semiquinone radical anions formed spontaneously in the alkaline solutions. For EPR/ENDOR measurements, cylindrical pyrex sample tubes with 3.5 mm o.d. (about 3.0 mm i.d.) were used. Solutions of the semiquinones in 2-propanol were generated from the quinones with a trace of benzoin and (usually) benzyltrimethylammonium hydroxide as base.

2.3. Instrumentation

EPR and ENDOR spectra were recorded on a Bruker ER-220D EPR spectrometer equipped with a Bruker cavity (ER-200ENB) and laboratory-built NMR facilities described elsewhere [8,9]. Typical experimental conditions: microwave power 1 mW and field modulation 5 μT in EPR measurements, microwave power 5 mW, radio-frequency power 55 W (corresponding to a field strength of $B_{RF} \approx 0.3$ mT in the rotating frame) and radio-frequency modulation ± 20 kHz at 10 kHz in ENDOR and EIE experiments. The temperature of the sample was adjusted by means of a temperature control unit Bruker VT-1000. The spectrometer was interfaced with a minicomputer (HP1000/A600) used for data acquisition in ENDOR experiments and handling and storage of the spectra. EPR spectra were accumulated by using a Nicolet 1170 signal-averager employing 1 K data points and afterwards transferred to the minicomputer. Alternatively, a Bruker ER-200D-SRC EPR spectrometer was used which was interfaced with a Comtec AT286/10 microcomputer via a MetraByte DAS-16 board. The microwave frequency was measured with an HP5245L/5255A frequency counter and the magnetic field strength ($B_0 \approx 0.34$ T) with a Bruker ER-035M NMR gaussmeter. In g-factor measurements, field gradients were corrected for by replacing the sample with a reference compound (phenalenyl in mineral oil, $g = 2.00262$).

2.4. Data Analysis

All spectra were transferred by PC-NFS to a local workstation (SUN SPARCstation IPC (4/40)). Spectra were evaluated by means of program DATA, yielding hyperfine couplings and linewidths from ENDOR spectra and an autocorrelation from EPR spectra. EPR spectrum simulations were performed on the workstation or on an AT-486 by means of the programs EPRFT, HFFIT or HFFITS. These programs (written by B.Kirste, programming language C) allow an iterative fitting of the digitized experimental spectra. All three programs treat isotropic hyperfine interaction to first order (high-field approximation). EPRFT assumes constant linewidths and performs the convolution of lineshape (Lorentzian, Gaussian or mixed Lorentzian-Gaussian) by means of Fourier transformation. Iterative fitting is

achieved alternatively by an evolutionary Monte Carlo method [10], by the simplex algorithm [11] or by the Marquardt procedure [12]. On the other hand, HFFIT and HFFITS allow for asymmetric linewidths, using the method of superimposing truncated lineshape functions; the Monte Carlo method serves for iterative fitting. Whereas HFFIT treats the M_I-dependence of linewidths in a simplified way (neglecting cross-terms, *vide infra*), HFFITS allows all linewidths to vary individually without any restriction by an underlying theory (adjusting intensities to keep areas constant). ENDOR spectra were simulated (deconvoluted) by means of program COMPASS written by E.Tränkle (Freie Universität Berlin, Institut für die Theorie der Elementarteilchen) using a VAXstation 3100.

For the conversion of units, the following relations are used: a [MHz] = 28.06 · a [mT] (g = 2.0048), a [mT] = 0.1 · a [G].

3. Results and Discussion

In Fig.1, the ENDOR spectrum of $1^{\ominus\ominus}$ recorded in 2-propanol is compared with those obtained in reversed-micellar solution. Whereas two ring protons are accidentally equivalent in 2-propanol (largest coupling), all major splittings are resolved in reversed-micellar solution (310 K). Hence five hyperfine coupling constants can be deduced from the separations of the respective line pairs which are centered about the free proton Larmor frequency (ν_H = 14.60 MHz). A tentative assignment of the fourth-largest coupling (4.67 MHz) to the two equivalent methylene protons (position 2β), based on ENDOR signal intensities and sign, has been confirmed by a computer simulation of the EPR spectrum (*vide infra*). It is noteworthy that the signals belonging to the second-largest coupling (6.76 MHz) are slightly but significantly broader than the others. A curve-fitting analysis (program COMPASS) yielded the following results for the peak-to-peak linewidths (given in parentheses), taking the average for low- and high-frequency signals: a_1 = − 7.19 MHz (98 kHz), a_2 = − 6.76 MHz (110 kHz), a_3 = − 4.95 MHz (91 kHz), a_4 = 4.67 MHz (103 kHz) and a_5 = 0.17 MHz (88 kHz). With decreasing temperature (290 K), the linewidths and their differences increase, but strong overlap of the signals prevents an accurate analysis.

For an assignment of the ring proton couplings to molecular positions, HMO/McLachlan calculations have been performed. Particular attention has been paid to the shifts of coupling constants observed in reversed-micellar solution as compared to the solution in 2-propanol. It is noteworthy that two ring proton couplings decrease in magnitude, whereas the third as well as the methylene proton coupling increase. Obviously, spin density is shifted from one part of the semiquinone radical anion to the other. Most likely this effect is caused by a change in solvation, particularly the strength of hydrogen bonding experienced by the two oxygen atoms. It is plausible that the

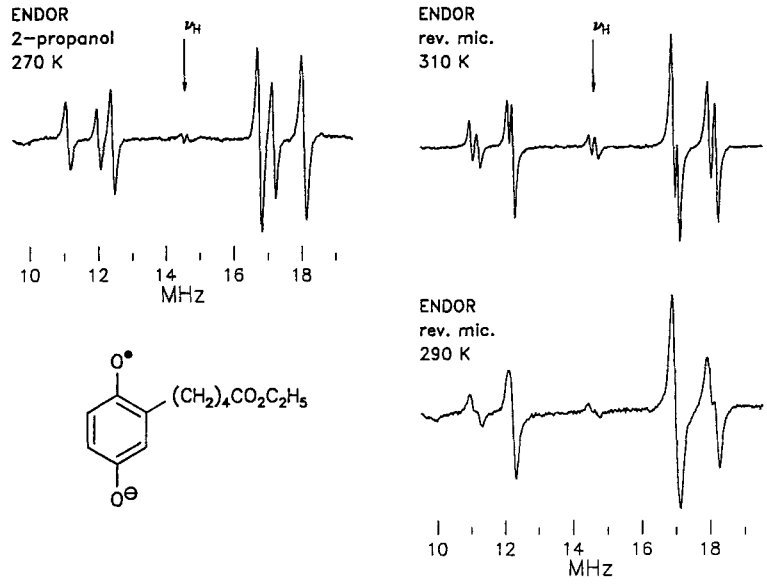

Fig.1. ENDOR spectra of $1^{\ominus\cdot}$ in 2-propanol (left) and in reversed-micellar solution (right).

apolar side chain will have an adverse effect on hydrogen bonding of the neighboring oxygen atom (O-1). Moreover, in reversed-micellar solution, this part of the molecule will tend to reside preferentially in the less polar interface region, whereas the other oxygen atom (O-4) should be surrounded by water molecules [3]. Consequently, negative *charge* will be shifted towards O-4, resulting in increased *spin* density at O-1. Within the scope of HMO/McLachlan calculations, this solvent effect can be taken into account by adjusting the Coulomb parameters, h_O, resulting in increased spin densities at positions 2 and 6 and decreased spin densities at positions 3 and 5. The corresponding assignment is given in Tables 1 and 2.

As a starting point for the HMO/McLachlan calculations, we used heteroatom parameters optimized for the 1,4-benzosemiquinone anion radical in alkaline aqueous solution: $h_O = 1.72$, $k_{OC} = 1.22$ and $Q_{CH}^{H} = -2.7\,\text{mT} = -75.9\,\text{MHz}$ [13]. The hyperconjugative model was employed for alkyl groups with parameters suggested for methyl groups ($h_{2a} = -0.1$, $h_{2b} = -0.5$, $k_{22a} = 0.7$, $k_{2a2b} = 2.5$) [14]. We then varied the values of the Coulomb parameters h_{O1} and h_{O4} to reflect changes of the medium, i.e. polarity and hydrogen-bonding capabilities; all other parameters were kept constant. The effect of hydrogen bonding will be an increase of the effective electronegativity at the oxygen atoms which can be expressed by an increased value of the Coulomb parameter h_O. Thus, h_O should be somewhat smaller in 2-propanol than in water. Moreover, alkyl groups are assumed to shield the neighboring oxygen atom, decreasing the strength of hydrogen

Table 1. Hyperfine coupling constants (MHz) of substituted 1,4-benzosemiquinone radical anions in 2-propanol.[a]

Compound	T (K)	a_2	a_3	a_5	a_6	$a(\gamma,\delta)$
1	260	+4.32	−5.18	−6.97	−6.97	−0.18
2	290	+4.66	−4.94	−7.02	−7.02	−0.14
3	290	+4.79	+4.79	−7.29	−7.29	
4	290	+6.24	−5.20	+6.24	−5.20	
5	290	+5.62	−5.62	−5.62	+5.62	
6	260	—	−6.03	+4.93	−5.47	−0.83(o,p),+0.50(m)
7	270	—	−6.58	+4.15	+5.04	−0.81(o,p),+0.51(m)
8	260	+3.92	−5.22	+5.95	−5.40	
9c	290	+3.16	−5.18	−6.83	−7.06	0.34
9t	290	+3.20	−5.18	−6.84	−7.07	0.37, 0.14
10c	280	+3.54	−5.35	+5.88	−5.35	0.38
10t	280	+3.46	−5.38	+5.84	−5.38	0.38
11c[b]	280	+3.25	−5.70	−5.30	+5.84	0.38
12t,I	260	—[c]	+5.03	−6.93	−7.49	0.37
12t,II	260	—[c]	+4.61	−6.32	−7.93	0.38
13	300	+6.54	−5.79	+0.09	+0.09	
14	290	+5.78	+2.94	+0.09	+0.09	−0.28
15,I	270	+0.65	+5.62	+0.08	+0.08	−0.39, +0.26
15,II	270	—[c]	+4.98	+0.08	+0.08	−0.51, +0.39
16c,I	270	+0.56	+5.83	+0.09	+0.09	−0.37, +0.26
16c,II	270	—[c]	+4.96	+0.08	+0.08	−0.49, +0.37
16t,I	270	+0.64	+5.88	+0.12	+0.12	−0.38, +0.26
16t,II	270	—[c]	+5.31	+0.12	+0.12	−0.47, +0.38

[a] Measured by ENDOR, accurate within ± 0.01 MHz. Signs were determined by general TRIPLE resonance. Numbering of molecular positions according to Scheme 1.
[b] Assignment to positions 3 and 5 uncertain.
[c] Small (≦ 0.5 MHz) but exact value not determined.

bonds because of their hydrophobic properties; this effect should be more pronounced for bulkier groups [3]. With the following choices, we could reproduce the experimental hyperfine data quite well, apart from a systematic error of about 0.2 MHz: the calculation for $\mathbf{1}^{\ominus\odot}$ in reversed micelles with $h_{O1} = 1.61$ and $h_{O4} = 1.72$ yields $a_3 = -4.81$ MHz, $a_5 = -6.46$ MHz, and $a_6 = -6.90$ MHz; for $\mathbf{1}^{\ominus\odot}$ in 2-propanol with $h_{O1} = 1.61$ and $h_{O4} = 1.68$, $a_3 = -5.06$ MHz, $a_5 = -6.69$ MHz, and $a_6 = -6.67$ MHz. Note that mainly the *differences* between h_{O1} and h_{O4} are crucial.

In Fig.2, EPR spectra of $\mathbf{1}^{\ominus\odot}$ in 2-propanol and in reversed-micellar solution are depicted along with computer simulations. Whereas all hyperfine components have the same width in 2-propanol solution, there is a pronounced asymmetric linewidth effect in reversed-micellar solution. This effect has already been observed and discussed in our previous study of semiquinones in reversed micelles [3].

Briefly, it is ascribed to slow-motional effects caused by anchoring of the semiquinone molecules at the interface between the water pool and the or-

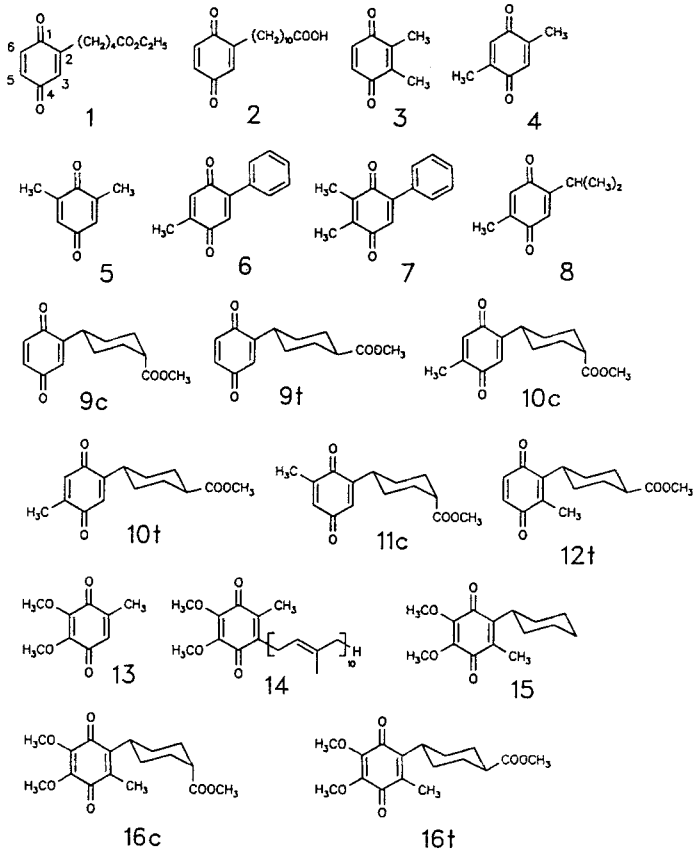

Scheme 1.

ganic bulk phase, constituted by surfactant molecules. For studies of radical mobility, also in reversed micelles [15–18], nitroxide spin probes have found by far the most wide-spread application. In the fast-tumbling (Redfield) regime, the asymmetric linewidth effect of nitroxide radicals can adequately be described by the following M_I-dependence [19]:

$$T_2^{-1} = A + BM_I + CM_I^2, \tag{1}$$

where B depends on the inner product of the **g**-tensor and the dipolar hyperfine tensor **A**′ (**g**′:**A**′) and C on (**A**′:**A**′); A depends on both (**g**′:**g**′) and (**A**′:**A**′) but is also influenced by field inhomogeneities, unresolved hyperfine splittings, exchange effects etc. and is usually less useful for linewidth analyses. Eq.(1) can be extended to the more general case of an electron spin interacting with several nonequivalent nuclei, but in this case cross-terms of

Table 2. Hyperfine coupling constants (MHz) of substituted 1,4-benzosemiquinone radical anions in reversed micelles.[a]

Compound	T (K)	a_2	a_3	a_5	a_6	$a(\gamma, \delta)$
1	310	+4.67	−4.95	−6.76	−7.19	−0.17
2	290	+4.76	−4.76	−6.84	−7.20	−0.16
3	300	+4.81	+4.81	−7.34	−7.34	
4	290	+6.43	−5.15	+6.43	−5.15	
5	290	+6.24	−5.15	−5.15	+6.24	
6	290	–	−5.78	+4.57	−5.78	−0.95(o,p), +0.53(m)
7	300	–	−6.04	+3.38	+5.74	−0.99(o,p), +0.56(m)
8	290	+4.26	−5.01	+5.89	−5.62	
9c	300	+3.70	−4.74	−6.48	−7.51	0.37
9t	290	+3.69	−5.06	−6.81	−7.19	0.37
10c	300	+4.04	−4.98	+5.71	−4.98	0.39
10t[b]	300	+3.94	−5.30	+5.95	−5.47	0.40
11c[c]	280	+4.07	−4.89	−4.48	+6.84	0.41
12t,II	300	–[d]	+4.45	−6.25	−8.14	0.38
13	290	+6.85	−5.55	+0.14	+0.14	
14	320	+5.55	+3.12	+0.08	+0.08	−0.29
15,I	300	+0.80	+5.35	+0.09	+0.09	−0.40, +0.27
15,II	300	–[d]	+4.76	+0.09	+0.09	−0.52, +0.37
16c,I	290	+0.69	+5.51	+0.08	+0.08	−0.36, +0.25
16c,II	290	–[d]	+5.33	+0.08	+0.08	−0.48, +0.36
16t,I	300	+0.73	+5.99	+0.10	+0.10	−0.36, +0.25
16t,II	300	–[d]	+5.23	+0.10	+0.10	−0.50, +0.36

[a] Measured by ENDOR, accurate within ± 0.01 MHz. Signs were determined by general TRIPLE resonance. Numbering of molecular positions according to Scheme 1.
[b] Assignment to positions 3 and 6 uncertain.
[c] Assignment to positions 3 and 5 uncertain.
[d] Small (≦ 0.5 MHz) but exact value not determined.

the type $E_{ij} M_{Ii} M_{Ij}$ depending on $(A_i' : A_j')$ also have to be taken into account [20,21]:

$$T_2^{-1} = A + \sum_i B_i M_{Ii} + \sum_i C_i M_{Ii}^2 + \sum_{\substack{i,j \\ i<j}} E_{ij} M_{Ii} M_{Ij} . \qquad (2)$$

Provided that one nucleus dominates the asymmetric line broadening, cross-terms should be negligible. We have employed the computer programs HFFIT and HFFITS for the simulation and iterative least-squares fitting of the EPR spectra [3]. In program HFFIT, all nuclei are treated independently, i.e., cross terms are not taken into account. Moreover, the C terms were not explicitly taken into account in the case of single nonequivalent protons ($M_I = \pm 1/2$) because their effect is experimentally indistinguishable from that of the A term. A typical example of a computer simulation based on this restricted model is depicted in Fig.2, bottom right. The match

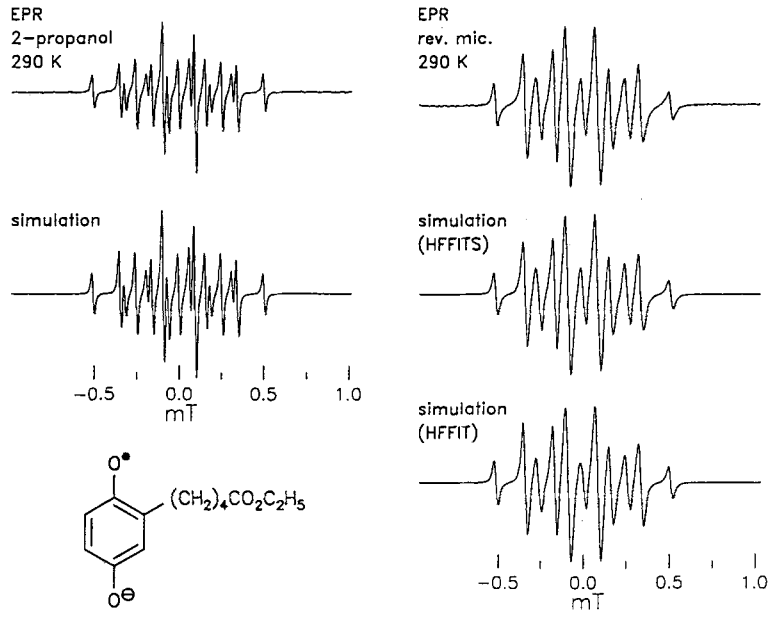

Fig.2. EPR spectra of $1^{\ominus\ominus}$ in 2-propanol and in reversed-micellar solution (top) as well as computer-simulated spectra (below). The EPR spectrum in reversed-micellar solution was simulated by two different methods: with individual optimization of linewidths (center right, program HFFITS) and by means of a simplified theoretical model of asymmetric line broadening neglecting cross terms (bottom right, program HFFIT), see text.

with the experimental spectrum (top right) is satisfactory but not perfect. A much better fit has been obtained by program HFFITS, allowing all linewidths to vary freely, see Fig.2, center right. In this case the coefficients of Eq.(2) were evaluated afterwards by multilinear regression analysis. Obviously, the neglect of the cross-terms is not really justified since theoretical estimates indicate that the inner products $(A_i':A_j')$ are comparable to $\mu_B B_0(g':A_i')$. Anyway, both methods agree that the dominant contribution to the asymmetric line broadening is due to the proton with the second-largest splitting (6.76 MHz).

According to the arguments presented above, this splitting should be assigned to ring position 5. It should be noted that the signals belonging to this proton also exhibit the largest linewidths in the ENDOR spectrum (*vide supra*). Following our discussion given previously [3], the particular role of this proton can be understood as follows. $1^{\ominus\ominus}$ is anchored with the ester side chain at the water-surfactant interface. Thus, rotations about the C_2–C_5 axis should remain essentially unaffected, whereas motions of this axis should be hindered. Since H-5 lies exactly on this axis, only anisotropies perpendicular to the C_5–H bond will be averaged out rapidly, whereas components along the bond direction are subject to slow-motional effects. According to the

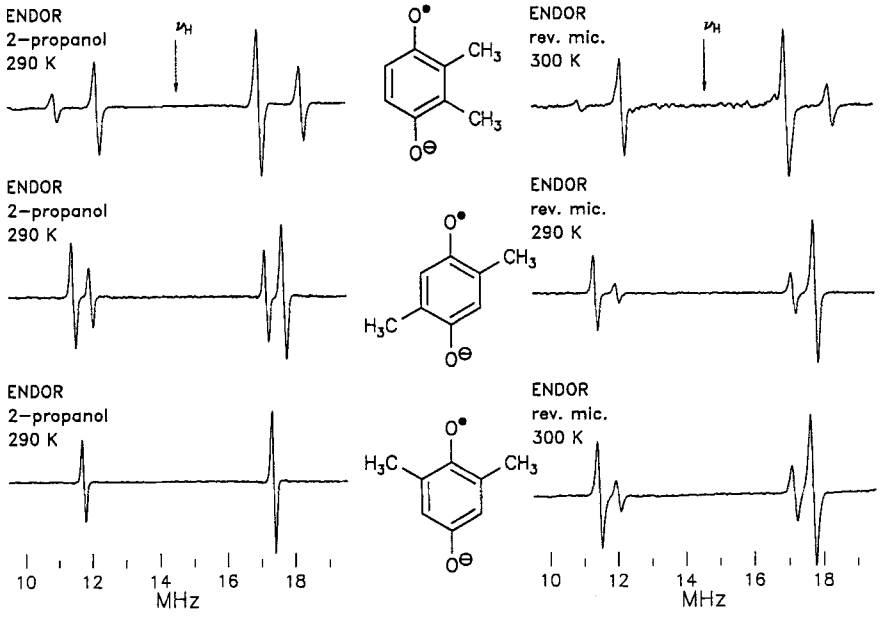

Fig.3. ENDOR spectra of isomeric dimethyl-1,4-benzosemiquinone radical anions in 2-propanol (left) and in reversed-micellar solution (right). Top to bottom: $3^{\ominus\odot}$, $4^{\ominus\odot}$ and $5^{\ominus\odot}$.

theory of McConnell and Strathdee, the largest component of the dipolar hyperfine tensor is just along the C–H bond axis [22].

An even longer side chain is present in $2^{\ominus\odot}$. As in the case of $1^{\ominus\odot}$, protons 5 and 6 are accidentally equivalent in 2-propanol but not in reversed micelles. There is also a pronounced asymmetric line broadening in reversed-micellar solution. In contrast to $1^{\ominus\odot}$, ENDOR and EPR spectra indicate that the contribution of proton 6 to this effect is almost as large as that of proton 5, see Table 4. It should be mentioned that the study of $2^{\ominus\odot}$ in reversed micelles proved to be more difficult. It is likely that the carboxyl group is responsible, forming a carboxylate anion in the alkaline solution. The behavior of this carboxylate group is open to question; it is unlikely to reside in the apolar part of the interface.

In Fig.3, ENDOR spectra of three isomeric dimethylbenzosemiquinones, $3^{\ominus\odot}$, $4^{\ominus\odot}$ and $5^{\ominus\odot}$, are compared. The hyperfine coupling constants are collected in Tables 1 and 2. In 2-propanol, ring and methyl protons of $5^{\ominus\odot}$ are accidentally equivalent. In the case of $3^{\ominus\odot}$ and $4^{\ominus\odot}$, the data obtained in 2-propanol and in reversed micelles are quite similar, differences are less than 0.2 MHz. On the other hand, the methyl proton coupling of $5^{\ominus\odot}$ increases by 0.6 MHz (10 %) in reversed-micellar solution, whereas the ring proton coupling decreases in magnitude by about the same amount (0.5 MHz). That means, a remarkable redistribution of spin density is found only

Table 3. *g*-values of selected 1,4-benzosemiquinone radical anions in 2-propanol and in reversed micelles.[a]

Compound	2-propanol	Rev. micelle
13	2.00469	2.00472
14	2.00469	2.00475
15,I	2.00465	2.00472
15,II	2.00470	2.00478
16c,I	2.00466	2.00475
16c,II	2.00474	2.00479
16t,I	2.00467	2.00470
16t,II	2.00471	2.00477

[a] Measured at 290 K, accuracy ± 0.00001.

in the compound which is unsymmetrically substituted with respect to the two oxygen atoms. Again, unsymmetrical solvation in reversed-micellar solution can explain this effect, with O-1 (between the methyl groups) attached to the water-surfactant interface and O-4 forming hydrogen bonds with water molecules in the pool. Although it is likely that the symmetrical compounds ($\mathbf{3}^{\ominus\odot}$ and $\mathbf{4}^{\ominus\odot}$) will also reside near the interface, reorientation must be rapid, providing an equivalent environment for the two oxygen atoms on the time average. However, it should be noted that preparation of reversed-micellar solutions is more difficult with symmetrical than with unsymmetrical semiquinones.

ENDOR spectra of two diastereomeric 2-(4-methoxycarbonylcyclohexyl)benzosemiquinone anions, $\mathbf{9c}^{\ominus\odot}$ (1e,4a or *cis* form) and $\mathbf{9t}^{\ominus\odot}$ (1e,4e or

Table 4. Linewidth asymmetry coefficients B (μT) of selected 1,4-benzosemiquinone radical anions in reversed micelles.[a]

Compound	T (K)	B_2	B_3	B_5	B_6
1	290	0.2	0.2	2.6	1.2
2	310	0.3	0.3	2.2	1.9
3	290	1.2	1.2	2.0	2.0
4	290	0.8	1.4	0.8	1.4
5	290	1.4	1.4	1.4	1.4
6	290	–	0.5	1.1	0.5
8	290	0.9	1.1	0.2	0.5
9c	290	1.4	1.2	2.5	1.2
9t	290	2.6	1.9	2.4	1.4
11c[b]	280	1.4	0.2	1.9	0.8
13	290	0.6	0.5	–	–
14	320	1.5	0.8	–	–

[a] The coefficients (cf. Eq.(2)) refer to peak-to-peak linewidths, first-derivative Lorentzian lineshape is assumed; determined by means of computer programs HFFIT or HFFITS.
[b] Assignment to positions 3 and 5 uncertain.

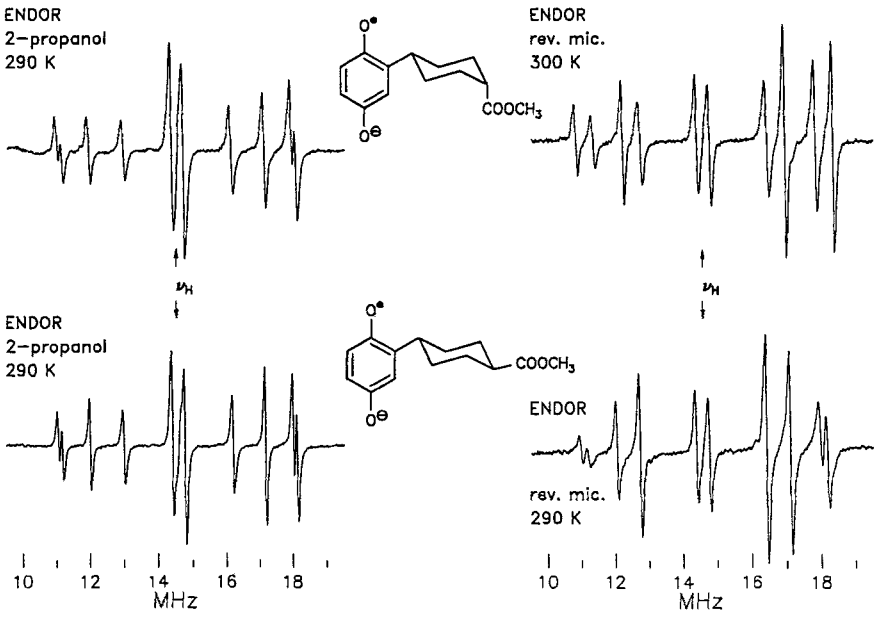

Fig.4. ENDOR spectra of two stereoisomers (a,e and e,e diastereomers), $\mathbf{9c}^{\ominus\odot}$ (top) and $\mathbf{9t}^{\ominus\odot}$ (bottom), in 2-propanol (left) and in reversed-micellar solution. Note that the spectra recorded in 2-propanol are virtually indistinguishable, whereas those in reversed micelles are clearly different.

trans form), are depicted in Fig.4. Whereas the spectra of the two stereoisomers are virtually indistinguishable in 2-propanol, there are pronounced differences in reversed-micellar solution (see Tables 1 and 2). Clearly, the remote ester group should not have any noticeable influence on the charge and spin distribution in the semiquinone moiety. Accordingly, $\mathbf{9c}^{\ominus\odot}$ and $\mathbf{9t}^{\ominus\odot}$ in 2-propanol exhibit essentially the same hyperfine couplings as the parent compound, 2-cyclohexylbenzosemiquinone [3]. In reversed-micellar solution, the behavior of the *cis* ester $\mathbf{9c}^{\ominus\odot}$ is quite similar to that of the parent compound with respect to hyperfine shifts and line-broadening effects, whereas the hyperfine shifts, referred to 2-propanol, are much smaller in the case of the *trans* ester **9t**. Although we cannot offer a definitive explanation for these differences, our suggestion is as follows. The *trans* ester has a more elongated shape than the other two compounds and might be anchored at the water-surfactant interface in such a way that the polarity of the environment of O-1 and O-4 is similar. In all three cases, the coupling of the 2β proton is about 0.5 MHz larger in reversed-micellar solution than in 2-propanol. This increase cannot solely be ascribed to a redistribution of spin density. According to the Heller-McConnell relation [23] and using 2-methylbenzosemiquinone as reference ($a_{Me} = 5.56$ MHz in 2-propanol, 5.85 MHz in reversed micelles), it can be accounted for by assuming a decrease of the (average) dihedral angle between the C–H_β bond and the

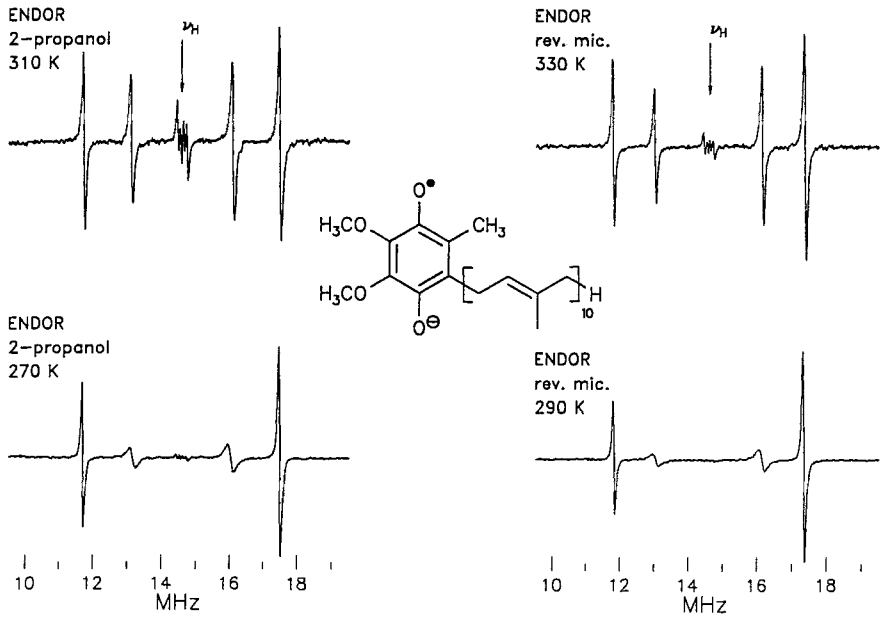

Fig.5. ENDOR spectra of ubisemiquinone-10 ($14^{\ominus\odot}$) at different temperatures in 2-propanol (left) and in reversed-micellar solution (right). Note that hindered rotation of the multiprenyl side chain gives rise to line broadening of the methylene proton signals at lower temperatures.

neighboring p_z orbital from 58° to 56°. A differentiation between diastereomers by ENDOR spectroscopy in reversed-micellar solution was also possible in the case of $\mathbf{10c}^{\ominus\odot}$ and $\mathbf{10t}^{\ominus\odot}$, carrying a methyl group in position 5 of the semiquinone moiety, see Table 2.

Ubiquinone-10 (**14**) is an interesting compound because of its biochemical relevance (coenzyme Q) and because of the long side chain (C_{50}) which seems to be a particularly well-suited anchor group for studies in reversed micelles. In fact, solutions of $\mathbf{14}^{\ominus\odot}$ in reversed micelles have been prepared without difficulty and proved to be fairly stable even at elevated temperatures (330 K). ENDOR spectra of $\mathbf{14}^{\ominus\odot}$ recorded in reversed micelles and in 2-propanol are depicted in Fig.5. It has long been known that the internal rotation of the multiprenyl side chain with respect to the semiquinone moiety is hindered, giving rise to a broadening and finally (at low temperatures) a splitting of the methylene proton ENDOR signals [24]. Actually, this broadening has been observed in both solvents dealt with in Fig.5; a splitting of signals did not occur within the accessible temperature range of reversed-micellar solutions (above 280 K). Das *et al.* have determined the activation energy for the hindered rotation in 1,2-dimethoxyethane, $E_a = 32$ kJ/mol ($\Delta H^{\ddagger} = 30$ kJ/mol) [24]. A rough analysis of the current data, based on actual saturated ENDOR linewidths without extrapolation to vanishingly small radio frequency and microwave powers [25], yielded the following estimates;

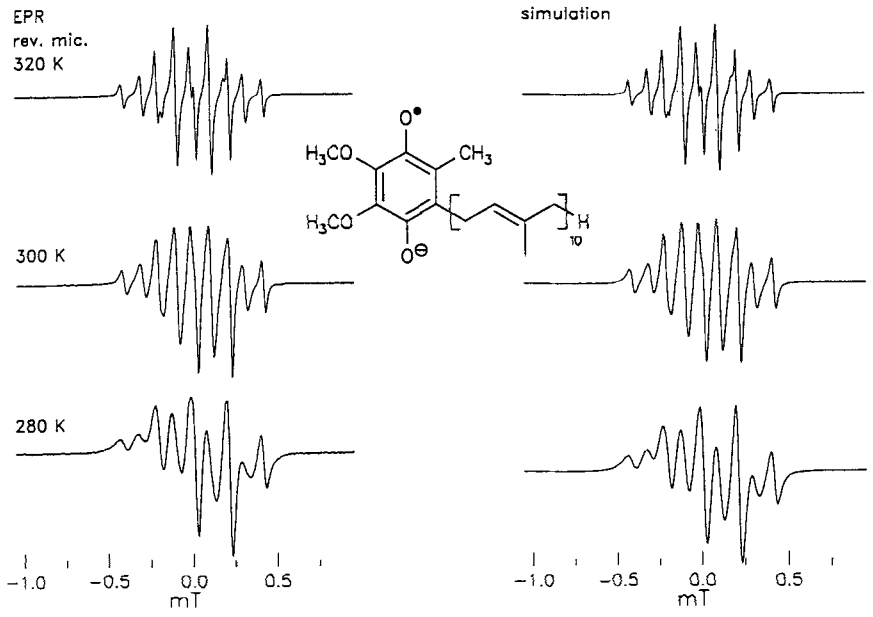

Fig.6. EPR spectra of ubisemiquinone-10 ($14^{\ominus\odot}$) at different temperatures in reversed-micellar solution (left) as well as computer simulations (right). In the simulations, linewidths were optimized individually (program HFFITS). Note that both asymmetric and alternating line broadening is present.

$14^{\ominus\odot}$ in 2-propanol: $\Delta H^{\ddagger} = 23\pm2$ kJ/mol, in reversed micelle: 33 ± 5 kJ/mol. The latter value might be in error, because it is not possible to differentiate between the two sources of additional line broadening, i.e. internal dynamics and slow molecular motion.

Figure 6 shows EPR spectra of $14^{\ominus\odot}$ in reversed micelles at different temperatures along with computer simulations (program HFFITS, individual optimization of linewidths). At 320 K, the *asymmetric* linewidth effect (due to slow molecular motion) dominates. Mainly the methylene protons contribute to this effect, but the influence of the methyl protons cannot be neglected ($B(CH_2) = 1.5$ μT, $B(CH_3) = 0.8$ μT). At 280 K, a pronounced *alternating* linewidth effect is observed, caused by the internal dynamics. In summary, it can be stated that $14^{\ominus\odot}$ is indeed an excellent probe molecule for studying the properties of the water-surfactant interface. As might be expected, the hyperfine shifts (referred to 2-propanol) indicate that the multiprenyl side chain serves as anchor group, evidently penetrating through the interface into the organic bulk phase. At the same temperature, the asymmetric line broadening is more pronounced than in the case of smaller semiquinones; it must be taken into account that only β protons are involved, which exhibit lower hyperfine anisotropies than α protons.

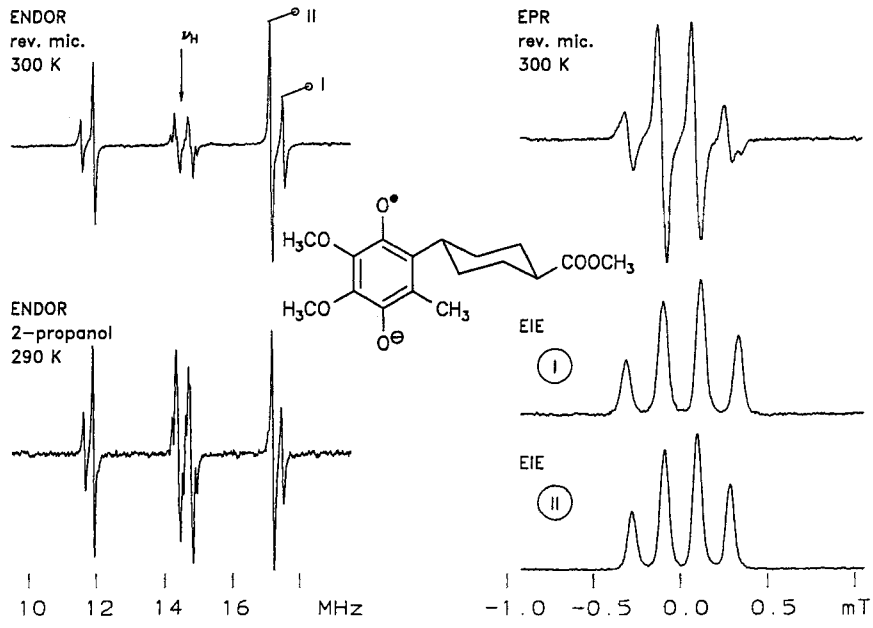

Fig.7. Left: ENDOR spectra of $\mathbf{16t}^{\ominus\odot}$ in reversed-micellar solution (top) and in 2-propanol (bottom). Right: EPR spectrum of $\mathbf{16t}^{\ominus\odot}$ in reversed-micellar solution (top) and ENDOR-induced EPR spectra obtained with two different radio-frequency settings, see the labels in the ENDOR spectrum (top left). Note that two different species are observed.

For comparison, ubisemiquinone-0 ($\mathbf{13}^{\ominus\odot}$), lacking the multiprenyl side chain, has been investigated. In this case the hyperfine shifts, reversed-micellar solution versus 2-propanol, are in the opposite direction, see Tables 1 and 2. Apparently the methyl group serves as anchor here. α and methyl protons contribute equally to the asymmetric linewidth effect observed in reversed micelles, see Table 4.

Furthermore, the three cyclohexyl derivatives $\mathbf{15}^{\ominus\odot}$, $\mathbf{16t}^{\ominus\odot}$ and $\mathbf{16c}^{\ominus\odot}$ have been studied. For example, EPR and ENDOR spectra of $\mathbf{16t}^{\ominus\odot}$ are depicted in Fig.7. At first sight, the ENDOR spectra might be interpreted in terms of cyclohexyl β and methyl proton couplings of almost equal magnitude. However, this interpretation is not in accordance with the EPR spectra, regarding the total splitting and the hyperfine pattern. Conclusive information was obtained by means of ENDOR-induced EPR (EIE) experiments, monitoring the ENDOR signals marked I or II in Fig.7, top left, while sweeping the magnetic field. The resulting EIE spectra are shown below the EPR spectrum (Fig.7, right). In both cases quartet patterns are obtained, but with different spacing and center (g-value). Consequently, ENDOR signals I and II must be due to different species. Further evidence has been gained from general TRIPLE experiments [9,26], since pumping of either signal I or II affects the signals in the center (near the free proton Larmor frequency)

quite distinctly. Moreover, ENDOR spectra of both species could be recorded selectively by carefully choosing the field position, i.e. the EPR component being desaturated; the high-field hyperfine component is sufficiently resolved for this purpose. It should be emphasized that these two species, although with somewhat different couplings, are observed both in reversed micelles and in 2-propanol. The ratio of the two species (I:II) is about 1:3, estimated from simulations of the EPR spectrum (in 2-propanol); I denotes the species with larger methyl proton coupling and smaller *g*-value (see Table 3).

Two species were also observed in the case of $\mathbf{15}^{\ominus\ominus}$ and $\mathbf{16c}^{\ominus\ominus}$, though with varying amounts and couplings, see Tables 1 and 2. For instance, "species I" dominates for $\mathbf{16c}^{\ominus\ominus}$ in 2-propanol (3:2), whereas the assignment in reversed micelles is uncertain. Furthermore, the isomeric cyclohexylmethylsemiquinones $\mathbf{10t}^{\ominus\ominus}$, $\mathbf{10c}^{\ominus\ominus}$, $\mathbf{11c}^{\ominus\ominus}$ and $\mathbf{12t}^{\ominus\ominus}$ shall be considered here. In the case of the 2,5- ($\mathbf{10t}^{\ominus\ominus}$, $\mathbf{10c}^{\ominus\ominus}$) and 2,6-isomers ($\mathbf{11c}^{\ominus\ominus}$), only a single species is found, whereas the 2,3-isomer ($\mathbf{12t}^{\ominus\ominus}$) gives rise to two species (see Table 1). Obviously sterical hindrance between neighboring cyclohexyl and methyl groups is responsible for this effect. Moreover, the cyclohexyl β proton coupling is quite different in these two types of compounds: between 3 and 4 MHz in the unhindered radicals, but less than 0.8 MHz in the hindered radicals exhibiting two species. Obviously the cyclohexyl β proton is forced into the plane of the semiquinone ring in the latter type. Of course, two different conformations fulfil this requirement; the β proton may point at the oxygen atom or at the methyl group. This would solve the puzzle of the two species.

Force-field calculations performed with the program ALCHEMY II (Tripos Associates) show indeed that these two conformations exhibit energy minima. The energy barrier is apparently not very high according to this model calculation (*ca.* 26 kJ/mol), suggesting that the interconversion should be fairly rapid. This prediction is not in accordance with the experiments, however, since up to about 340 K two distinct species are observed. However, the force-field calculation does not take solvation effects into account, and solvent reorganization might give a major contribution to the energy barrier.

4. Conclusions

We have demonstrated that reversed micelles provide a suitable medium for EPR and ENDOR studies of semiquinones. Since this environment is quite similar to biological membranes, it is very attractive for studies of biologically relevant molecules such as ubiquinone. Shifts of hyperfine coupling constants, referred to those measured in ordinary solvents (e.g. 2-propanol), and the analysis of asymmetric linewidth effects allow conclusions with respect to location and fixation of the semiquinone radical anions at the water-surfactant interface of the reversed micelles. Moreover, we have shown that the selectivity of this binding even allows the differentiation between stereoisomers (diastereomers).

Acknowledgements

We thank Mrs. E.Brinkhaus for her assistance in recording EPR spectra, H.Dieks, Th.Stabingis, A.Wiehe and Dr. H.Hungerbhler for generously supplying us with several quinone samples, Priv.-Doz. Dr. E.Tränkle for making available his program COMPASS and Dr. M.Plato (Freie Universität Berlin, Institut für Molekülphysik) for many helpful discussions. B.K. and H.K. gratefully acknowledge financial support by the Fonds der Chemischen Industrie and the Deutsche Forschungsgemeinschaft (Normalverfahren and SFB 337).

References

[1] Trumpower B.L. (ed.): Function of Quinones in Energy Conserving Systems. New York: Academic Press 1982.
[2] Boxer S.G.: Biochim. Biophys. Acta **726**, 265 (1983); Wasielewski M.R.: Photochem. Photobiol. **47**, 923 (1988); von Gersdorff J., Huber M., Schubert H., Niethammer D., Kirste B., Plato M., Möbius K., Kurreck H., Eichberger R., Kietzmann R., Willig F.: Angew. Chem. **102**, 690 (1990); Angew. Chem., Int. Ed. Engl. **29**, 670 (1990); Lendzian F., Schlüpmann J., von Gersdorff J., Möbius K., Kurreck H.: Angew. Chem. (in press).
[3] Niethammer D., Kirste B., Kurreck H.: J. Chem. Soc., Faraday Trans. **86**, 3191 (1990)
[4] Luisi P.L.: Angew. Chem. **97**, 449, (1985); Angew. Chem., Int. Ed. Engl. **24**, 439 (1985)
[5] Jacobsen N., Torssell K.: Justus Liebigs Ann. Chem. **763**, 135 (1972)
[6] Dieks H., Kurreck H.: to be published.
[7] Langlais M., Buzas A., Freon P.: C. R. Hebd. Séances Acad. Sci. **254**, 1452 (1962)
[8] Kurreck H., Kirste B., Lubitz W.: Angew. Chem. **96**, 171 (1984); Angew. Chem., Int. Ed. Engl. **23**, 173 (1984)
[9] Kurreck H., Kirste B., Lubitz W. in: Electron Nuclear Double Resonance Spectroscopy of Radicals in Solution. New York: VCH Publishers 1988.
[10] Kirste B.: J. Magn. Reson. **73**, 213 (1987)
[11] Nelder J.A., Mead R.: Computer J. **7**, 308 (1965); Beckwith A.L.J., Brumby S.: J. Magn. Reson. **73**, 252 (1987)
[12] Marquardt D.W., Bennett R.G., Burrell E.J.: J. Mol. Spectrosc. **7**, 269 (1961); Marquardt D.W.: J. Soc. Ind. Appl. Math. **11**, 431 (1963)
[13] Sullivan P.D., Bolton J.R., Geiger W.E. Jr.: J. Am. Chem. Soc. **92**, 4176 (1970)
[14] Lazdins D., Karplus M.: J. Am. Chem. Soc. **87**, 920 (1965)
[15] Lim Y.Y., Fendler J.H.: J. Am. Chem. Soc. **100**, 7490 (1978)
[16] Barelli A., Eicke H.-F.: Langmuir **2**, 780 (1986)
[17] Häring G., Luisi P.L., Hauser H.: J. Phys. Chem. **92**, 3574, (1988)
[18] Kotake Y., Janzen E.G.: J. Phys. Chem. **92**, 6357, (1988)
[19] Nordio P.L. in: Spin Labeling. Theory and Applications (Berliner L.J. ed.), vol.1, p.5. New York: Academic Press, Inc. 1976.
[20] Freed J.H., Fraenkel G.K.: J. Chem. Phys. **39**, 326 (1963)
[21] Hudson A., Luckhurst G.R.: Chem. Rev. **69**, 191 (1969)
[22] McConnell H.M., Strathdee J.: Mol. Phys. **2**, 129 (1959)
[23] Heller H.C., McConnell H.M.: J. Chem. Phys. **32**, 1535 (1960)
[24] Das M.R., Connor H.D., Leniart D.S., Freed J.H.: J. Am. Chem. Soc. **92**, 2258 (1970)
[25] Reference [9], Chapter 6.
[26] Biehl R., Plato M., Möbius K.: J. Chem. Phys. **63**, 3515 (1975)

Author's address: Prof. Dr. Harry Kurreck, Institut für Organische Chemie Freie Universität Berlin, Takustr.3, D-1000 Berlin 33, Germany